Instability of channel flow with oscillatory wall suction/blowing

Peng Gao and Xi-Yun Lu[a)]
Department of Modern Mechanics, University of Science and Technology of China, Anhui, Hefei 230026, China

(Received 22 June 2005; accepted 14 February 2006; published online 29 March 2006)

The stability of channel flow modulated by oscillatory wall suction/blowing is investigated using linear stability analysis together with Floquet theory based on numerical calculation and asymptotic expansion. Two typical flows with either the driven pressure gradient or the flow rate constant are considered. The basic flows subject to the oscillatory wall suction/blowing are time periodic with multiple frequency components. The stability problem is formulated into a time-dependent eigenvalue problem, and the Floquet exponents are obtained using a spectral collocation method. It is revealed that the periodic wall suction/blowing induces the Stokes layer, which interacts with the disturbance shear wave and eventually affects the disturbance growth. Results show that the modulations of the oscillatory wall suction/blowing to the channel flows have a destabilizing effect and the similar stability characteristics of both the typical flows occur. Critical Reynolds numbers and wave numbers are predicted for a wide range of parameters. Asymptotic expansions of the growth rate at small amplitude Δ of the oscillatory wall suction/blowing are developed. The correction terms for the growth rate occur in $O(\Delta^2)$ and are positive, indicating that the flow is destabilized. It is found that the destabilizing effect is mainly connected to the steady corrections of the mean flow profile in the $O(\Delta^2)$ terms. © *2006 American Institute of Physics*.
[DOI: 10.1063/1.2186673]

I. INTRODUCTION

The stability of channel flow subject to various modifications is of great importance in fundamentals and applications. Orszag[1] obtained the critical Reynolds number of plane Poiseuille flow, $R_c=5772.22$, using expansions in Chebyshev polynomials to approximate the solutions of the Orr-Sommerfeld equation. Then, a variety of investigations have been devoted to the effects of various modifications on the stability of the primary plane Poiseuille flow. These modifications typically include surface roughness,[2–4] wavy or vibrating walls,[5–8] uniform or distributed surface suction,[9,10] and so on. On the other hand, the wall suction/blowing is proved to be one of the most effective ways in laminar-turbulent transition control[11–13] and turbulence control.[14–17]

The stability characteristics of the flow may be changed significantly due to the effects of the wall suction/blowing. As is well known, the asymptotic suction boundary layer is much more stable than the Blasius boundary layer.[18,19] Generally, the wall suction/blowing is usually associated with stabilizing/destabilizing the flow in the sense of hydrodynamic stability. Hains[20] first performed the linear stability analysis of channel flow with suction at the lower wall and injection at the upper wall driven by a constant pressure gradient along the streamwise direction, and revealed that the cross flow has a stabilizing effect. Sheppard[21] also carried out similar work using a Galerkin method and confirmed the results of Hains. Recently, Fransson and Alfredsson[9] studied the similar problem with either the flow rate or the maximum streamwise velocity constant, and found that the cross flow has a destabilizing effect in certain parameter regions and a stabilizing effect for others.

Further, the stability of time-periodic flows, which has been reviewed by Davis,[22] also exists extensively in a variety of problems. The stability of oscillatory plane Poiseuille flow, relevant to the present study, is a typical problem of the stability of time-periodic flows. Grosch and Salwen[23] first used the Galerkin method and Floquet theory to investigate the stability characteristics of the oscillatory plane channel flow, and found that the periodic modulated pressure gradient has a stabilizing effect on the flow near the critical point of the underlying steady flow when the values of the ratio of oscillation velocity amplitude to the mean velocity amplitude are less than 0.105. Herbert[24] then examined the energy balance in modulated plane Poiseuille flow in the thin Stokes layers near the wall by extending Lin's work.[25] He emphasized the interactions between the Stokes layers caused by the modulation and the disturbance shear wave, and derived that if the thickness of the disturbance shear wave relative to that of the modulation shear wave is greater than 1/2, the modulation stabilizes the flow. Hall[26] found that the high frequency modulations have a slightly destabilizing effect. Furthermore, von Kerczek[27] analyzed this stability problem by a perturbation method and demonstrated that the flow is more stable at moderate frequencies and more unstable at very low and very high frequencies. However, he did not find any strongly unstable modes, in conflict with the results of Grosch and Salwen.[23] Recently, Singer, Ferziger, and Reed[28] reexamined this stability problem via direct numerical simulations of the Navier-Stokes equations and two-dimensional linear simulations. They indicated that the maximum growth

[a)]Author to whom correspondence should be addressed. Electronic mail: xlu@ustc.edu.cn.

rates occur when there are large regions of positive curvature near each wall and suspected the lack of resolution of the Stokes layers for the results of Grosch and Salwen.[23] Straatman *et al.*[29] also performed the linear stability analysis of channel flow modulated by an oscillatory pressure gradient, as a model of the physiologically pulsatile flow, for an extensive range of parameters.

However, the effects of oscillatory wall suction/blowing on the stability of channel flow studied here are still unclear but are highly desired. It is necessary to mention that the present problem is different from those concerning the effects of spatial modulations, such as spatially distributed wall suction/blowing and a wavy wall.[2–8] If a nonzero phase velocity of the wall is prescribed, a wavy wall with small amplitude can be modeled in the first order by a wall suction/blowing, which is periodic both in space and time,[7] while the vanishing of the phase velocity reduces the normal velocity component at the wall to be zero. The wall suction/blowing considered here is periodic in time and uniform in space, so that centrifugal instability[5] or flow separation[8] disappears.

Our goal in this study is to assess how the oscillatory wall suction/blowing affects the stability characteristics of plane Poiseuille flow. Since the basic flow is periodic in time, Floquet theory[30] is used to represent the solutions. In the present study, two typical flows, either driven by a constant pressure gradient or constrained by a fixed flow rate are considered. The corresponding stability problem is formulated into a time-dependent eigenvalue problem, and the stability characteristics of the flows are obtained using a numerical calculation and an asymptotic analysis.

The rest of this paper is organized as follows. The numerical and asymptotic results of the basic flow are given in Sec. II. The governing equations and methods of the stability problem based on the numerical calculation and asymptotic perturbation are described in Sec. III. The results for the stability characteristics are discussed in Sec. IV. Finally, a summary is provided in Sec. V.

II. CHANNEL FLOW WITH OSCILLATORY WALL SUCTION/BLOWING

In this section, the mean channel flow modulated by unsteady wall suction/blowing is obtained using a numerical method and an asymptotic expansion. Then the results will be applied to the stability analysis numerically and theoretically, respectively.

A. Basic flow

Considering the incompressible Newtonian fluid with the density ρ and kinematic viscosity ν bounded by two infinite parallel porous plates, the schematic of the flow configuration together with the coordinate system is exhibited in Fig. 1. The distance between the upper and lower boundaries is $2\bar{H}$, and an oscillatory suction/blowing on the channel walls is employed in the form

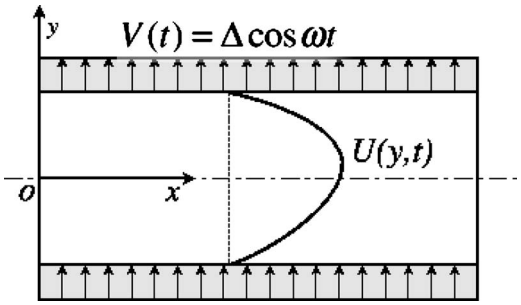

FIG. 1. Schematic of the flow configuration.

$$\bar{V}_w = \bar{\Delta}\cos\bar{\omega}\bar{t}, \tag{1}$$

where the overbar means dimensional variables, $\bar{\Delta}$ and $\bar{\omega}$ are the amplitude and frequency of the oscillatory suction/blowing, respectively. We take $\bar{H}$ as the length scale, the centerline velocity $\bar{U}_c$ of the Poiseuille flow without suction/blowing modulation as the velocity scale, and $\rho\bar{U}_c^2$ as the pressure scale. Then, two typical Reynolds numbers, R and R_v, can be defined and described as, respectively,

$$R = \bar{U}_c\bar{H}/\nu, \quad R_v = \bar{\Delta}\bar{H}/\nu.$$

The corresponding dimensionless amplitude and frequency of the suction/blowing are $\Delta = R_v/R$ and $\omega = \bar{\omega}\bar{H}/\bar{U}_c$, respectively.

Assuming the periodic basic flow has the form

$$U = U(y,t), \quad V = \Delta\cos\omega t, \quad W = 0, \quad P = Gx, \tag{2}$$

which satisfies the continuity equation automatically. Then, substituting them into the Navier-Stokes equations gives the governing equation for the streamwise velocity,

$$\frac{\partial U}{\partial t} + \Delta\cos\omega t\frac{\partial U}{\partial y} = -G + \frac{1}{R}\frac{\partial^2 U}{\partial y^2}, \tag{3}$$

where G is the pressure gradient in the streamwise direction. Here, we consider two constraint conditions, which can be chosen as the pressure gradient either constant or time dependent to keep the flow rate fixed, i.e.,

$$G(t) = \begin{cases} -\dfrac{2}{R}, & \text{for constant pressure gradient;} \\ \dfrac{1}{2R}\dfrac{\partial U}{\partial y}\Big|_{-1}^{1}, & \text{for fixed flow rate.} \end{cases} \tag{4}$$

The no-slip condition is applied at the walls, i.e.,

$$U(\pm 1,t) = 0. \tag{5}$$

Since the problem (3)–(5) has no analytical solutions, a numerical approach must be employed. Considering the channel flow driven by the constant pressure gradient as a typical case, the streamwise velocity can be expressed as

$$U(y,t) = \sum_{n=-\infty}^{\infty} A_n(y) e^{in\omega t}, \tag{6}$$

where $i=\sqrt{-1}$ and $A_n(y)=A_{-n}^*(y)$ in order for U to be real. Here, an asterisk denotes a complex conjugate. Substituting Eq. (6) into Eq. (3) and separating Fourier components, we obtain

$$\left(in\omega - \frac{1}{R}D^2\right)A_n + \frac{\Delta}{2}D(A_{n-1} + A_{n+1}) = \frac{2}{R}\delta_{n0}, \tag{7}$$

where $D=\partial/\partial y$, and δ_{ij} is the Kronecker delta. The boundary conditions corresponding to Eq. (5) have the form $A_n(\pm 1)=0$. Approximate solutions can be obtained by truncating Eq. (6) to M leading Fourier modes and solving a coupled system of $2M+1$ ordinary differential equations of Eq. (7). Note that the condition $A_n(y)=A_{-n}^*(y)$ can be used to reduce the system to $M+1$ equations. Here, this approach has not been used because the time cost for computing the basic flow is nearly negligible. Instead, this property is employed for verifying the accuracy of the present calculations. The spatial derivatives are discretized using the Chebyshev spectral collocation method and represented by the corresponding differentiation matrices. Then the augmented matrix system possesses a block-tridiagonal property and can be inverted efficiently.

The validation of the Fourier truncation method depends on the rate of convergence of the Fourier series, which means that the energy of the modes is damped quickly as their frequencies increase. The relative importance of mode n can be assessed by calculating its energy E_n which is defined as

$$E_0 = \frac{1}{4}\int_{-1}^{1} |A_0|^2 \, dy, \tag{8}$$

$$E_n = \frac{1}{2}\int_{-1}^{1} |A_n|^2 \, dy (n > 0). \tag{9}$$

Variations of energy of the first five modes as a function of the amplitude Δ for $R=5000$ and $\omega=0.2$ are shown in Fig. 2. It demonstrates that the series converge very rapidly for the amplitude Δ considered here. Typically 5 to 10 modes, which can ensure the calculation accuracy, are used for the calculations in the present study.

Note that the introduction of the oscillatory wall suction/blowing would decrease the flow rate with respect to that of the pure plane Poiseuille flow driven by the same constant pressure gradient. This feature has been also found in the channel flow subject to constant suction[9] or spatially periodic suction.[3] Alternatively, a fixed flow rate can be maintained by varying the pressure gradient in Eq. (4). To obtain the streamwise velocity, an additional condition

$$\int_{-1}^{1} U(y,t) dy = \frac{4}{3} \tag{10}$$

should be set to keep the flow rate of the channel flow modulated by the oscillatory suction/blowing to be identical to that of plane Poiseuille flow without any modulation. Here, it is

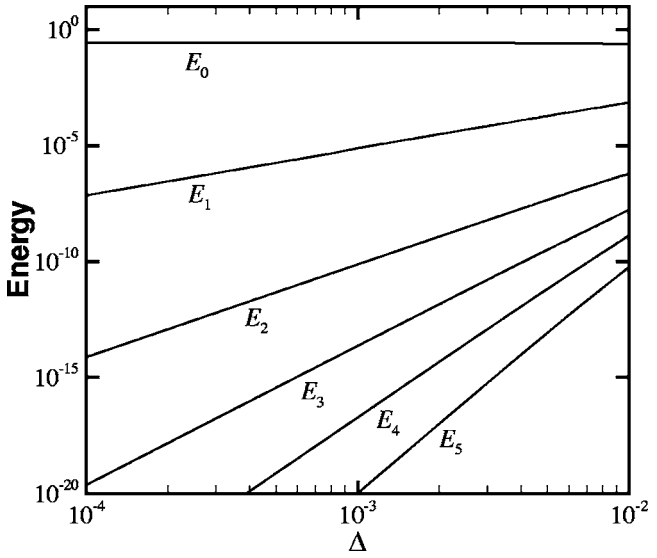

FIG. 2. Variations of the energy for the basic flow versus the amplitude Δ for $R=5000$ and $\omega=0.2$.

helpful to introduce a new variable $\Psi(y,t)$, which is related to $U(y,t)$ by

$$U(y,t) = \frac{\partial \Psi}{\partial y} + \frac{2}{3}, \tag{11}$$

where the constant $2/3$ is added only for the purpose of simplifying the boundary conditions for Ψ. Taking $\partial/\partial y$ of Eq. (3) to eliminate the pressure gradient and substituting Eq. (11) into the resulting equation, we have the following equation for Ψ:

$$\frac{\partial^3 \Psi}{\partial t \partial y^2} + \Delta \cos(\omega t)\frac{\partial^3 \Psi}{\partial y^3} = \frac{1}{R}\frac{\partial^4 \Psi}{\partial y^4}, \tag{12}$$

and the boundary conditions are

$$\Psi(\pm 1,t) = Q, \quad \frac{\partial \Psi}{\partial y}(\pm 1,t) = -\frac{2}{3}, \tag{13}$$

where Q is a constant and $Q=0$ is used here for convenience. The periodic solution of Eq. (12) together with Eq. (13) can be solved by a similar numerical method used in solving the streamwise velocity for the channel flow driven by constant pressure gradient. Once Ψ is obtained, the streamwise velocity U can be solved from Eq. (11).

The typical variation of the mean velocity during one period is shown in Fig. 3 for the case of constant pressure gradient at $R=5000$, $R_v=20$, and $\omega=0.2$. It is needed to indicate that the mean velocity for the case of a fixed flow rate (not shown here) has a similar property. As shown in Fig. 3(a), the maximum of U is less than one, which represents the decrease of the flow rate. Figure 3(b) shows the difference of the mean flow modulated by the oscillatory wall suction/blowing and that of the plane Poiseuille flow. We can identify the presence of the Stokes layers near the walls, which are caused by the oscillatory wall modulation. The decrease of the flow rate can be confirmed by

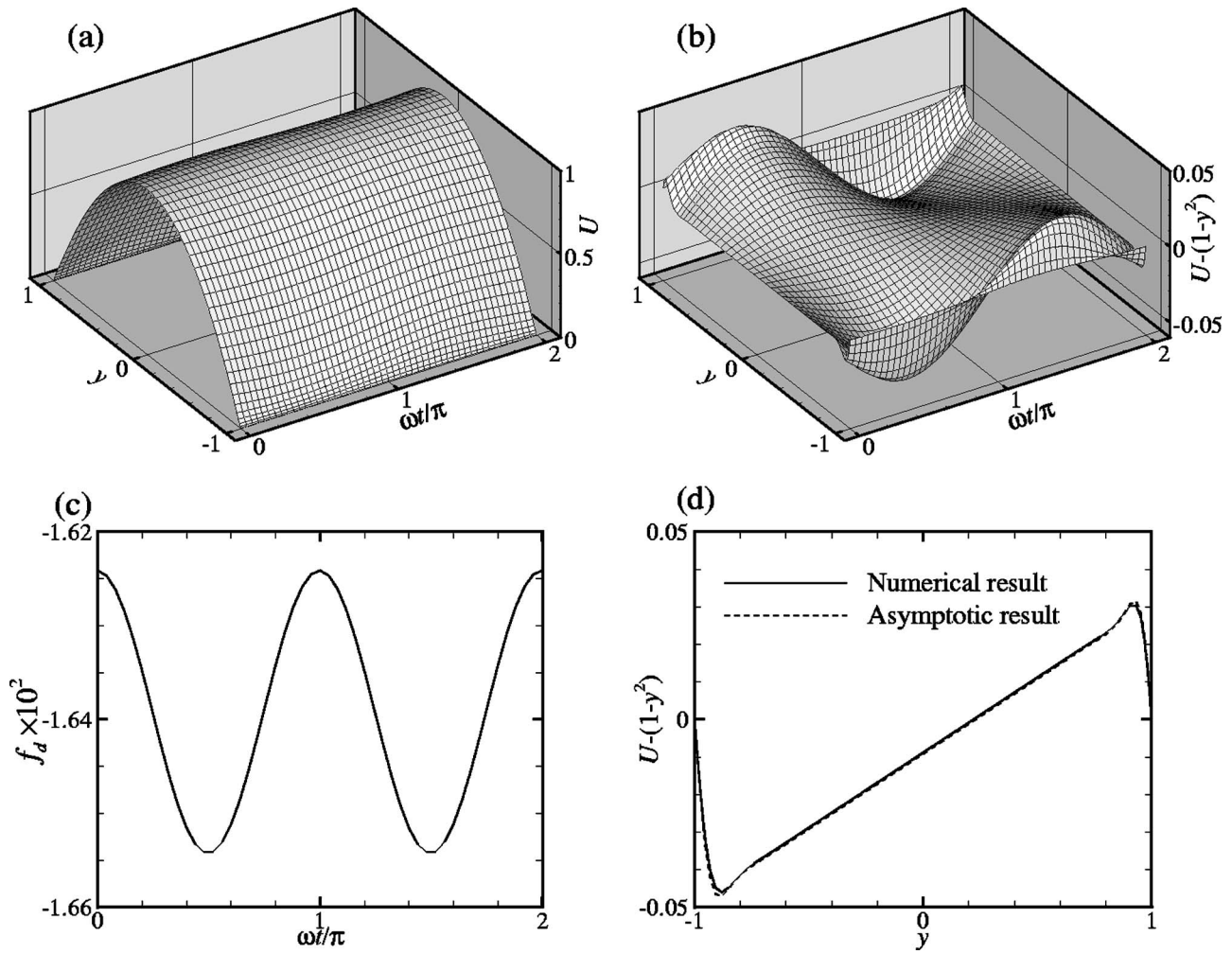

FIG. 3. Properties of the basic flow for the case of a constant pressure gradient at $R=5000$, $R_v=20$ ($\Delta=4\times10^{-3}$) and $\omega=0.2$. (a) A mesh plot of U; (b) $U-(1-y^2)$; (c) the difference of the flow rate of the modulated channel flow and that of the pure Poiseuille flow; (d) a comparison of the asymptotic and numerical results of $U-(1-y^2)$ at $\omega t=\pi/2$.

$$f_d(t)=\int_{-1}^{1}U(y,t)dy-\frac{4}{3}, \tag{14}$$

which is shown in Fig. 3(c), where a negative value of f_d is exhibited.

B. Asymptotic solution

Suppose that the oscillatory wall suction/blowing is sufficiently weak, i.e., the amplitude of the modulation is small enough compared with the characteristic scale of the streamwise mean velocity; then the mean flow can be expanded as

$$U(y,t)=U_0(y,t)+U_1(y,t)\Delta+U_2(y,t)\Delta^2+O(\Delta^3). \tag{15}$$

Here, we first consider the channel flow driven by the constant pressure gradient. Substituting Eq. (15) into Eqs. (3) and (5) and collecting terms corresponding to each power of Δ, we obtain the following system of perturbation equations:

$$\frac{\partial U_0}{\partial t}-\frac{1}{R}\frac{\partial^2 U_0}{\partial y^2}=\frac{2}{R}, \tag{16}$$

$$\frac{\partial U_1}{\partial t}-\frac{1}{R}\frac{\partial^2 U_1}{\partial y^2}=-\cos\omega t\frac{\partial U_0}{\partial y}, \tag{17}$$

$$\frac{\partial U_2}{\partial t}-\frac{1}{R}\frac{\partial^2 U_2}{\partial y^2}=-\cos\omega t\frac{\partial U_1}{\partial y}, \tag{18}$$

and the corresponding boundary conditions are described as

$$U_n(\pm1,t)=0,\quad n=0,1,2. \tag{19}$$

The solution of Eqs. (16) and (19) gives nothing but the parabolic velocity profile of the pure plane Poiseuille flow, which is independent of time, i.e.,

$$U_0(y)=1-y^2. \tag{20}$$

Further, the solution of Eqs. (17) and (19) must have the form

$$U_1(y,t)=U_{11}(y)e^{i\omega t}+U_{12}(y)e^{-i\omega t}, \tag{21}$$

and

$$U_{11}(y)=\frac{R}{\beta^2}\left(y-\frac{\sinh\beta y}{\sinh\beta}\right), \tag{22}$$

$$U_{12}(y) = U_{11}^{*}(y), \tag{23}$$

where $\beta = \sqrt{i\omega R} = (1+i)/\delta$, with δ being the dimensionless thickness of the Stokes layer induced by the oscillatory wall suction/blowing. In a similar way, the solution of Eqs. (18) and (19) is obtained to be

$$U_2(y,t) = U_{20}(y) + U_{21}(y)e^{2i\omega t} + U_{22}(y)e^{-2i\omega t}, \tag{24}$$

and

$$U_{20}(y) = \frac{R^2}{2\beta^3}\left(\coth\beta - \frac{\cosh\beta y}{\sinh\beta}\right) + \text{c.c.}, \tag{25}$$

$$U_{21}(y) = \frac{R^2}{2\beta^3}\left[\left(\frac{1}{2\beta} - \coth\beta\right)\frac{\cosh\sqrt{2}\beta y}{\cosh\sqrt{2}\beta} - \left(\frac{1}{2\beta} - \frac{\cosh\beta y}{\sinh\beta}\right)\right], \tag{26}$$

$$U_{22}(y) = U_{21}^{*}(y), \tag{27}$$

where c.c. denotes the complex conjugate. It is easy to prove that the steady component U_{20} is always negative and causes the decrease of the flow rate.

If the flow rate is specified to be constant, the approximate solution Ψ of Eq. (12) combined with Eq. (13) can also be obtained. Then, the streamwise mean velocity, which is expressed as Eq. (15), can be derived through Eq. (11). As the leading-order and first-order components of U are the same as Eq. (20) and (20), the only difference occurs in the second-order component with its coefficients in the form

$$U_{20}(y) = \frac{R^2}{4\beta^3}\left((1-y^2)\frac{3}{\beta} + (3y^2-1)\coth\beta - 2\frac{\cosh\beta y}{\sinh\beta}\right) + \text{c.c.}, \tag{28}$$

$$U_{21}(y) = \frac{R^2}{\beta^3}(A\cosh\beta y + B\cosh\sqrt{2}\beta y + C), \tag{29}$$

$$U_{22}(y) = U_{21}^{*}(y), \tag{30}$$

where

$$A = \frac{1}{2\sinh\beta}, \quad B = \frac{\sinh\beta - \beta\cosh\beta}{2\beta\cosh\sqrt{2}\beta - \sqrt{2}\sinh\sqrt{2}\beta},$$

$$C = \frac{\coth\beta - \sqrt{2}\coth\sqrt{2}\beta}{2\sqrt{2}\beta\coth\sqrt{2}\beta - 2}.$$

Since both $U_{11}(y)$ and $U_{12}(y)$ are odd functions, which cannot contribute to the change of the flow rate, it is not surprising to note that the expansions of U up to $O(\Delta)$ has the same formulation for the channel flows subject to both the constraint conditions. It will be discussed in Sec. IV that U_{20} plays an important role to the stability of the channel flows modulated by the oscillatory wall suction/blowing. The variation of U_{20} for $R=5772.22$ and $\omega=0.2$ is shown in Fig. 4. It is observed that the obvious difference of U_{20} for both the channel flows occurs. Here, it is needed to indicate that these asymptotic results are valid, provided that

$$\frac{R_v}{\sqrt{\omega R}} \ll 1. \tag{31}$$

The comparison between the asymptotic and numerical velocity profiles for the channel flow driven by constant pressure gradient is shown in Fig. 3(d) for $R=5000$, $R_v=20$, and $\omega=0.2$. It is observed that the asymptotic solution agrees well with the numerical result, although $R_v/\sqrt{\omega R}=0.63$ is not small enough to satisfy Eq. (31). For smaller R_v, the asymptotic profile coincides with the numerical result very well.

III. STABILITY PROBLEM

The stability analysis of the channel flow modulated by the oscillatory wall suction/blowing is studied by numerical calculation and asymptotic analysis, coupled with the Floquet theory, owing to the periodic character of the basic flow.

A. Formulation

The basic state (2) is infinitesimally disturbed as follows:

$$(u,v,w,p) = (U,V,W,P) + (u',v',w',p')\varepsilon, \tag{32}$$

where $|\epsilon| \ll 1$. Substituting Eq. (32) into the Navier-Stokes and continuity equations with a linearizing process and eliminating the pressure, we obtain the governing equation for the disturbances, which takes the form

$$\left[\left(\frac{\partial}{\partial t} + U\frac{\partial}{\partial x} + VD\right)\nabla^2 - D^2U\frac{\partial}{\partial x}\right]v' = -\frac{1}{R}\nabla^4 v'. \tag{33}$$

Since U and V depend on y and t only, Eq. (33) can be separated in x and z, and thus each mode can be considered separately. Then, the wave-like solutions are introduced as

$$v'(x,y,z,t) = \hat{v}(y,t)e^{i(\alpha x+\gamma z)} + \text{c.c.}, \tag{34}$$

where α and γ are real and denote the streamwise and spanwise wave numbers, respectively. Substituting Eq. (34) into Eq. (33) results in

$$\left[\left(\frac{\partial}{\partial t} + i\alpha U + VD\right)(D^2-k^2) - i\alpha D^2U\right]\hat{v} = \frac{1}{R}(D^2-k^2)^2\hat{v}, \tag{35}$$

where $k^2=\alpha^2+\gamma^2$. The boundary conditions at the walls are

$$\hat{v}(\pm 1,t) = D\hat{v}(\pm 1,t) = 0. \tag{36}$$

Here, Eq. (35) represents the time-dependent Orr-Sommerfeld (OS) equation with additional terms due to the mean normal velocity V.

There is a Squire's theorem guaranteeing that the critical Reynolds number occurs for a two-dimensional disturbance for steady shear flow. This theorem is also valid for the unidirectional unsteady shear flow in which separate time and length scales are defined, such as the oscillatory Stokes layers.[31] For the mean flow considered here, which is not parallel shear flow anymore, it can be proved in a similar way that any three-dimensional disturbance is related to a

two-dimensional one at lower R and higher ω for fixed values of R_v. Thus, only two-dimensional disturbances will be examined, i.e., $\gamma=0$.

Since the basic flow is periodic with the period $T=2\pi/\omega$, according to the Floquet theory, we expect that the solutions of Eq. (35) have the form

$$\hat{v}_j(y,t) = e^{\mu_j t}\phi_j(y,t) \quad (j=1,2,\dots), \tag{37}$$

where ϕ_j are periodic in time with the same period T of the basic flow and μ_j are complex numbers called Floquet exponents. Note that these modes are ordered in such a way that ascending values of j, starting with $j=1$, correspond to descending values of $\mathrm{Re}(\mu_j)$. Then μ_1 will be the Floquet exponent with the largest real part. The basic flow is mentioned to be asymptotically stable to infinitesimal disturbances if $\mathrm{Re}(\mu_1)<0$ and unstable if $\mathrm{Re}(\mu_1)>0$.

For the channel flow modulated by the oscillatory wall suction/blowing considered here, there exists a useful symmetry property. By introducing the transformation

$$y' = -y, \quad t' = t + T/2, \tag{38}$$

it is identified that no change occurs in the form of the problem (3). Therefore, we obtain

$$U(y,t) = U(-y, t+T/2). \tag{39}$$

In a similar way, the transformation, Eq. (38), does not change the form of Eq. (35) and the boundary conditions, Eq. (36), for $\hat{v}$. Thus, we can conclude that if $\hat{v}(y,t)$ is a solution of Eq. (35), so is $\hat{v}(-y,t+T/2)$. This property will allow us to infer the solutions for the time interval $[0,T]$ from these for $[0,T/2]$ in the numerical analysis later.

B. Numerical procedure

Equation (35) is discretized in the wall-normal direction using a Chebyshev spectral collocation technique with the Gauss-Lobatto collocation points

$$y_j = \cos\frac{j\pi}{N+1} \quad (j=0,\dots,N+1).$$

The discrete operators are compiled using the spectral MATLAB Differentiation Matrix Suite developed by Weideman and Reddy,[32] which has been recently used to study a variety of hydrodynamic stability problems.[33,34]

Now the semidiscretized OS equation can be represented by a set of ordinary equations, which have the form

$$\frac{d\mathbf{f}}{dt} = A(t)\mathbf{f}, \tag{40}$$

where $\mathbf{f}(t)=[\hat{v}(y_1,t),\dots,\hat{v}(y_N,t)]^T$ and $A(t)$ is a periodic N-by-N matrix with the period T. To obtain the Floquet exponents, we should consider a generalization of Eq. (40),

$$\frac{dF}{dt} = A(t)F, \tag{41}$$

where F is an N-by-N matrix of solution vectors. Using the Floquet theorem, we expect the fundamental matrix of Eq. (41) to have the form

$$F(t) = P(t)e^{tQ}, \tag{42}$$

where P is a T-periodic matrix in t and Q is a constant matrix, whose eigenvalues are just the Floquet exponents μ_j. Without any loss of generality, the initial value of F can be taken to be an identity matrix, i.e.

$$F(0) = I. \tag{43}$$

Further, we can obtain

$$F(T) = e^{tQ}. \tag{44}$$

Then the Floquet exponents μ_j can be solved from the eigenvalues σ_j of $F(T)$ by

$$\mu_j = \frac{1}{T}\ln\sigma_j \quad (j=1,\dots,N). \tag{45}$$

The integration of Eq. (41) to obtain $F(T)$ is performed with the fourth-order Runge-Kutta method.

It is shown that the symmetry property of the basic flow discussed in Sec. III A can be employed to simplify the numerical calculation. First, we define a new matrix,

$$F_c(t) = I_c F(t), \quad t\in[0,T], \tag{46}$$

where I_c is an N-by-N matrix in which the entries $a_{ij}=\delta_{i+j,N+1}$ and satisfies

$$I_c^2 = I. \tag{47}$$

Applying to another matrix, $I_c F$ gives F with the row j and row $N-j+1$ interchanged for j from 1 to $N/2$. Then we define another new matrix,

$$F_1(t) = F(t)F^{-1}(T/2)I_c, \quad t\in[T/2,T], \tag{48}$$

which is also a solution of Eq. (41) as this set of equations is homogeneous. Since

$$F_1(T/2) = I_c = F_c(0), \tag{49}$$

we obtain

$$F_1(T) = F(T)F^{-1}(T/2)I_c = F_c(T/2), \tag{50}$$

according to the symmetry property. Hence,

$$\begin{aligned} F(T) &= F_c(T/2)[F^{-1}(T/2)I_c]^{-1} = F_c(T/2)I_c^{-1}F(T/2) \\ &= F_c(T/2)I_cF(T/2) = F_c^2(T/2). \end{aligned} \tag{51}$$

Thus Eq. (41) needs to be integrated only over $0\leqslant t\leqslant T/2$, and the overall computational cost is halved. Furthermore, there is even no need to calculate explicitly the value of $F(T)$. Let κ_j denote the eigenvalues of $F_c(T/2)$, then according to Eq. (51), it is easy to prove that σ_j can be obtained from

$$\sigma_j = \kappa_j^2. \tag{52}$$

The reliability of Eqs. (51) and (52) has been verified by our numerical results. Certainly, they can also serve to validate our code.

The results of numerical tests listed in Table I exhibit the accuracy of numerical solutions. We can find that even $N=30$ gives acceptable results. It is noted that the results for $M=1$ demonstrate an obvious error, indicating the impor-

tance of high-frequency components of the basic flow. Generally, more Fourier modes and Chebyshev collocation points are needed for higher amplitude Δ and lower frequency ω of the modulation. Typically $N=40$ to 50, $M=5$ to 10 are used in our calculations.

C. Asymptotic analysis

The basic flows considered are modulated about a nonzero mean flow, in contrast with the pure oscillatory flows, e.g., the Stokes layers. Thus the effect of the modulation on the stability characteristics of the flow can be evaluated, similar to the approach proposed by Hall,[26] using perturbation methods when the oscillatory components are small compared to the mean flow. So, in addition to the numerical calculation shown previously, the results of the system specified by Eqs. (35) and (36) can be obtained from an alternative method by expanding the Floquet exponents and eigenfunctions in the form

$$\mu_j = \mu_{j0} + \mu_{j1}\Delta + \mu_{j2}\Delta^2 + \cdots, \tag{53}$$

$$\phi_j(y,t) = \phi_{j0}(y) + \phi_{j1}(y,t)\Delta + \phi_{j2}(y,t)\Delta^2 + \cdots, \tag{54}$$

for sufficiently small Δ. Upon substituting Eqs. (15) and (37) and $V=V_1\Delta$ into Eq. (35), collecting terms of equal powers in Δ, we obtain a series of equations in y and t.

The equation of the leading order is just the time-independent OS equation that governs the stability of the pure plane Poiseuille flow and reads as

$$\mu_{j0}(D^2-\alpha^2)\phi_{j0} - L_{os}\phi_{j0} = 0, \tag{55}$$

where the linear OS operator is defined as

$$L_{os} \equiv i\alpha D^2 U_0 - i\alpha U_0(D^2-\alpha^2) + \frac{1}{R}(D^2-\alpha^2)^2. \tag{56}$$

The eigenfunctions ξ_{j0} of the adjoint equation of Eq. (55),

$$(\mu_{j0}^* - i\alpha U_0)(D^2-\alpha^2)\xi_{j0} - 2i\alpha\, DU_0\, D\xi_{j0} = \frac{1}{R}(D^2 - \alpha^2)^2\xi_{j0} \tag{57}$$

will be needed. It is known that ξ_{j0} are orthogonal to ϕ_{j0} by the biorthogonality condition

$$\int_{-1}^{1} \xi_{j0}^*(D^2-\alpha^2)\phi_{i0}\, dy = \delta_{ij}; \tag{58}$$

we suppose here that the eigenfunctions have been normalized.

Considering the first-order correction, the governing equation is

$$\left(\frac{\partial}{\partial t} + \mu_{j0}\right)(D^2-\alpha^2)\phi_{j1} - L_{os}\phi_{j1} = i\alpha\, D^2U_1\, \phi_{j0} - (\mu_{j1} + i\alpha U_1 + V_1 D)(D^2-\alpha^2)\phi_{j0}. \tag{59}$$

Since the right-hand side of Eq. (59) contains only terms $\sin\omega t$, $\cos\omega t$, and terms independent of t, we can assume the period solution as

$$\phi_{j1}(y,t) = \phi_{j10}(y) + \phi_{j11}(y)e^{i\omega t} + \phi_{j12}(y)e^{-i\omega t}. \tag{60}$$

Substituting Eq. (60) into Eq. (59) yields

$$\mu_{j0}(D^2-\alpha^2)\phi_{j10} - L_{os}\phi_{j10} = -\mu_{j1}(D^2-\alpha^2)\phi_{j0}, \tag{61}$$

and

$$(\mu_{j0}+i\omega)(D^2-\alpha^2)\phi_{j11} - L_{os}\phi_{j11} = i\alpha D^2U_{11}\phi_{j0} - (i\alpha U_{11} + V_{11}D)(D^2-\alpha^2)\phi_{j0}, \tag{62}$$

$$(\mu_{j0}-i\omega)(D^2-\alpha^2)\phi_{j12} - L_{os}\phi_{j12} = i\alpha D^2U_{12}\phi_{j0} - (i\alpha U_{12} + V_{12}D)(D^2-\alpha^2)\phi_{j0}, \tag{63}$$

where U_{11} and U_{12} have been obtained in Sec. II B, and $V_{11}=V_{12}=1/2$ so that $V_1(t)=V_{11}e^{i\omega t}+V_{12}e^{-i\omega t}=\cos\omega t$. In order to keep that Eq. (61) has a solution, the right-hand side must satisfy the orthogonality condition

$$-\mu_{j1}\int_{-1}^{1}\xi_{j0}^*(D^2-\alpha^2)\phi_{j0}\, dy = -\mu_{j1} = 0, \tag{64}$$

i.e., $\mu_{j1}=0$, which means that the effect of the oscillatory wall suction/blowing with amplitude Δ on the disturbance growth rate occurs only of order Δ^2. It is reasonable to note that the change of the sign of Δ does not alter the stability character of the flow.

Since $\mu_{j1}=0$, we must advance the solutions to the next order to obtain μ_{j2} the real part of which, if it exists, shall determine the characteristics of the stability. The governing equation for the second-order correction is

$$\left(\frac{\partial}{\partial t} + \mu_{j0}\right)(D^2-\alpha^2)\phi_{j2} - L_{os}\phi_{j2} = -(\mu_{j2} + i\alpha U_2)(D^2-\alpha^2)\phi_{j0} + i\alpha\, D^2U_2\, \phi_{j0} - (i\alpha U_1 + V_1 D)(D^2-\alpha^2)\phi_{j1} + i\alpha\, D^2U_1\, \phi_{j1}. \tag{65}$$

Assuming the solution has the form

$$\phi_{j2}(y,t) = \phi_{j20}(y) + \phi_{j21}(y)e^{2i\omega t} + \phi_{j22}(y)e^{-2i\omega t}, \tag{66}$$

we obtain the equation for ϕ_{j20}, which has the form

$$\mu_{j0}(D^2-\alpha^2)\phi_{j20} - L_{os}\phi_{j20} = -\mu_{j2}(D^2-\alpha^2)\phi_{j0} + \chi_{j1} + \chi_{j2} + \chi_{j3}, \tag{67}$$

where

$$\chi_{j1} = i\alpha\, D^2U_{12}\, \phi_{j11} - i\alpha U_{12}(D^2-\alpha^2)\phi_{j11} + i\alpha\, D^2U_{11}\, \phi_{j12} - i\alpha U_{11}(D^2-\alpha^2)\phi_{j12}, \tag{68}$$

$$\chi_{j2} = i\alpha\, D^2U_{20}\, \phi_{j0} - i\alpha U_{20}(D^2-\alpha^2)\phi_{j0}, \tag{69}$$

$$\chi_{j3} = -\tfrac{1}{2}(D^3 - \alpha^2 D)(\phi_{j11} + \phi_{j12}). \tag{70}$$

Note that ϕ_{j11} and ϕ_{j12} can be solved from Eqs. (62) and (63), respectively. Then the solvability condition of Eq. (67) yields

$$\mu_{j2} = M_{j1} + M_{j2} + M_{j3}, \tag{71}$$

where

$$M_{jn} = \int_{-1}^{1} \xi_{j0}^{*} \chi_{jn}\, dy \quad (n = 1,2,3). \tag{72}$$

We can reasonably divide the terms contributing to μ_{j2} into M_{j1}, M_{j2} and M_{j3}, which express the contributions of the first-order correction of the streamwise mean flow, the steady part of the second-order correction of the streamwise mean flow, and the normal mean flow, respectively. Such a division allows us to investigate separately the effect of each factor on the stability in the following section.

The variables in Eqs. (68)–(70) are obtained by solving the corresponding equations with the Chebyshev collocation method. Gauss-Lobatto quadrature is used to compute μ_{j2} to ensure the high accuracy.

IV. RESULTS

Our calculations show that there are no qualitative differences of the stability characteristics for the channel flows subject to the constraint with either constant pressure gradient or fixed flow rate, respectively. Thus, we discuss mainly on the case of the constant pressure gradient and briefly on the case of the fixed flow rate in Sec. IV D.

A. Accuracy of the calculations

In addition to the symmetry property, i.e., Eq. (51), which can serve as a verification of our numerical calculations, there are a number of checks on the results of the calculation. By setting $\Delta=0$, the Floquet exponents should coincide with the growth rate of the disturbance modes of plane Poiseuille flow. For $\alpha=1$, $R=10\,000$, our calculation with $N=50$ gives the growth rate of the most unstable mode

$$\mathrm{Re}(\mu_1) = 3.739\,669 \times 10^{-3}.$$

Further, we also obtain the critical Reynolds number $R_c = 5772.22$, corresponding to a wave number $\alpha_c = 1.020\,56$. These results are in quite good agreement with those predicted by Orszag.[1]

The validation of our results can also be proved by the comparison of the numerical and asymptotic results later.

B. Stability property at $R=R_c$ and $\alpha=\alpha_c$

There exist four dimensionless parameters, α, R, R_v, and ω, in this problem. Calculations are carried out in which the disturbance wave number α and the Reynolds number R are specialized while both the amplitude and frequency of the oscillatory wall suction/blowing vary. Typically, it is of interest to study first the effects of the imposed modulation on the disturbance modes of the steady flow at the critical point $\alpha=\alpha_c=1.020\,56$, $R=R_c=5772.22$.

First we hold ω constant, which is chosen to be comparable to the frequency of the neutrally stable mode at the critical point ($\omega_1=0.2694$), and change R_v. The growth rate of the most unstable mode for various values of ω_1/ω is shown in Fig. 5, where $\mathrm{Re}(\mu_1)$ is plotted as a function of R_v. Generally, the disturbance becomes more unstable as R_v increases from zero. However, note that, at $\omega_1/\omega=2$, there exists an intersecting point, which represents that the eigenvalue corresponding to the most unstable mode changes from one mode's eigenvalue to the other one and the intersection of the curves for the most unstable modes occurs. At $\omega_1/\omega=2$, the growth rate is negative around $R_v=45$, indicating that the disturbance wave at the critical point is stabilized. However, it does not mean that the flow is stabilized by the modulation, since we can probe later that there exist other unstable disturbances at a lower Reynolds number. It can also be found that the flow is strongly unstable for low frequency but slightly unstable for high frequency.

To further investigate the effect of the frequency, typical calculations, in which R_v is kept constant while ω varies, are carried out. The results are shown in Fig. 6, where the growth rate $\mathrm{Re}(\mu_1)$ is plotted as a function of ω_1/ω. Note that the amplitude of the first-order correction of the basic

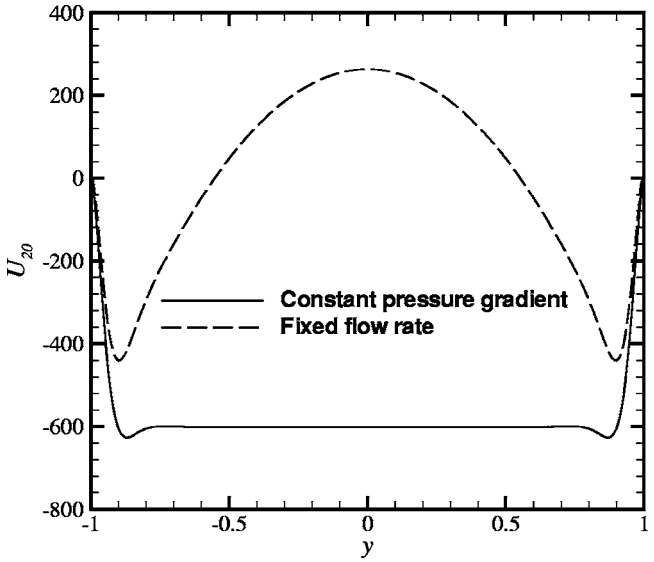

FIG. 4. Variation of U_{20} for $R=5772.22$ and $\omega=0.2$.

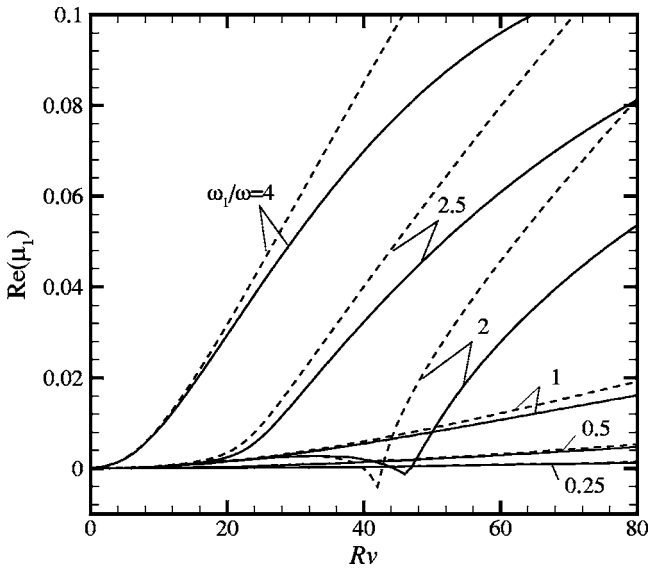

FIG. 5. Profiles of the principal disturbance growth rate $\mathrm{Re}(\mu_1)$ as a function of R_v for various values of ω at $R=5772.22$, $\alpha=1.020\,56$.——, constant pressure gradient;——fixed flow rate.

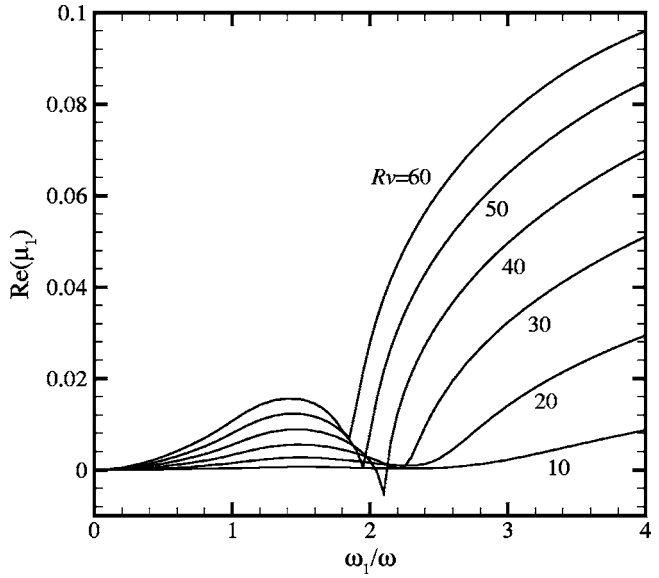

FIG. 6. Profiles of the principal disturbance growth rate $\mathrm{Re}(\mu_1)$ as a function of ω_1/ω for various values of R_v at $R=5772.22$, $\alpha=1.020\,56$.

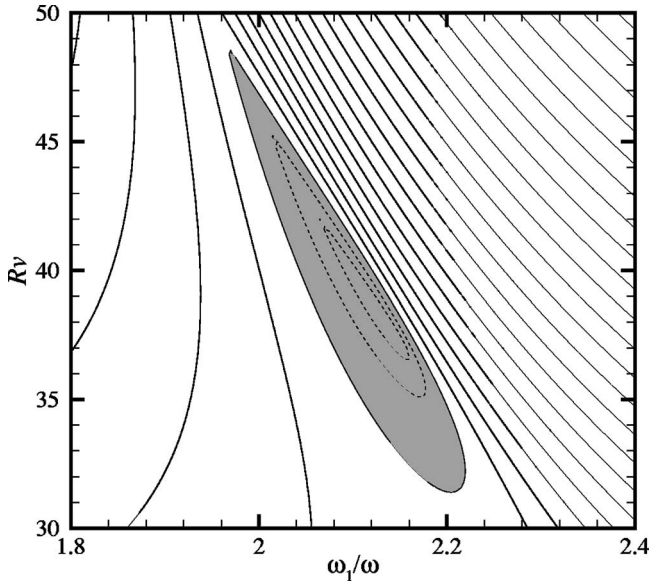

FIG. 7. Contour of the growth rate of the most unstable mode $\mathrm{Re}(\mu_1)$ at $R=5772.22$, $\alpha=1020\,56$. Dashed contour lines and gray area represent negative values. The contour interval is 0.002.

flow, which is given by $U_1\Delta$, is proportional to R_v/ω for fixed R, according to Eqs. (22) and (23). For high frequencies, the modulation of the mean flow due to the oscillatory wall suction/blowing is weak and has only a slightly destabilizing effect. The growth rate of the most unstable mode increases as ω_1/ω increases from zero and reaches a local maximum value at $\omega_1/\omega\approx 1.5$. Increasing ω_1/ω (or reducing ω) further causes the decrease of $\mathrm{Re}(\mu_1)$, and even stabilizes the disturbance mode around $R_v=40$. At $\omega_1/\omega\approx 2$, different properties of the curves occur, depending on the values of R_v. For $R_v<30$, the growth rate increases smoothly as ω_1/ω increases, while the intersecting points are formed for $R_v>30$. When ω tends to zero, the basic flow is strongly affected by the modulation and the growth rate of the most unstable disturbance wave increases rapidly when ω_1/ω increases. Hence the flow is strongly unstable for the low frequencies studied. When the frequency becomes small further, the number of the time step needed to take numerically integrating the equations in one period increases rapidly, resulting in the calculations being much more expansive. Since the channel flow with a steady wall suction/injection is more stable,[9,20,21] it is reasonably predicted that, according to the quasistatic theory, that the flow can eventually be stabilized as ω tends to zero.

Figures 5 and 6 also indicate the presence of a certain parameter region, in which the neutral mode at (α_c, R_c) is stabilized. The contour of the growth rate of the most unstable mode $\mathrm{Re}(\mu_1)$ plotted in the $R_v-\omega_1/\omega$ plane is shown in Fig. 7. The neutral mode can be stabilized for the parameters R_v and ω_1/ω in a limited region, indicated by the gray area. The minimum and maximum values of R_v in the gray region are 31.4 and 48.5, respectively, i.e., the wall suction/blowing has only a destabilizing effect on the neutral mode for $R_v<31.4$ or $R_v>48.5$.

To probe the behavior at the intersecting point, it is needed to calculate more eigenvalues around the point. Figure 8 shows the real part of the first four Floquet exponents as a function of ω_1/ω for several values of R_v. When ω approaches infinity (or ω_1/ω to zero), the modification of the mean flow is negligible. Thus, the Floquet exponents may tend to the eigenvalues μ_{j0} for the parabolic velocity profile of the pure plane Poiseuille flow, which are listed in Table II. Here, we first consider the behavior of the second and third modes shown in Fig. 8. It is observed that the profiles of the second and third modes are approaching together. However, the eigenfunctions are obviously different, as exhibited in Table II. The second mode is antisymmetric with respect to the centerline $y=0$, while the third mode is symmetric. Meanwhile, the curves of the second and third modes are nearly unchanged versus ω_1/ω; it means that the second and third modes of the plane Poiseuille flow are almost unaffected by the modulation. This character may be explained by the following two reasons. Note that the eigenvalues of the second and third modes have large imaginary parts, which indicate high disturbance frequency (≈ 0.9735). First, if the frequency of oscillatory wall suction/blowing is as high as the disturbance frequency, the modulation of the mean flow is too weak to affect the disturbance, and the imposed Stokes layer is too closely confined to the boundaries to have an effect on the disturbance. Second, if the frequency is low, there may be a large mismatch between the mode and the disturbance frequency.

However, as shown in Fig. 8, the first and fourth modes are strongly affected by the modulation. At $R_v=10$, the curve for each eigenvalue does not intersect. At $R_v=20$, the fourth mode becomes the second most unstable in the range $1.9<\omega_1/\omega<2.8$. The corresponding range increases as R_v increases. Meanwhile, by viewing the curves at $R_v=30$ and 35, the local minimum value of the real part of the first eigenvalue and the local maximum value of the real part of the fourth eigenvalue approach gradually together and the curves become varying sharply at $\omega_1/\omega\approx 2.15$. At $R_v=40$, it is interesting to note that both the first and fourth modes have

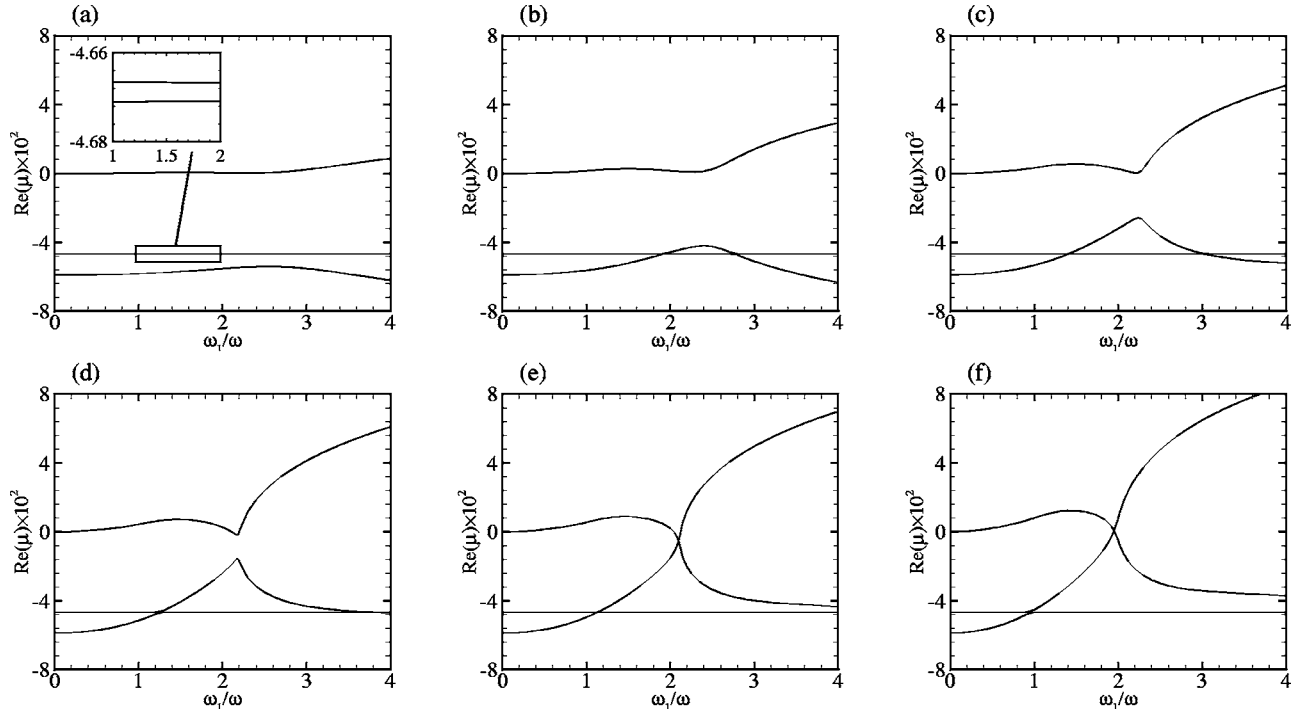

FIG. 8. Profiles of the real part of the first four principal Floquet exponents as a function of ω_1/ω for several values of R_v at $R=5772.22$, $\alpha=1.020\,56$. (a) $R_v=10$, (b) 20, (c) 30, (d) 35, (e) 40, (f) 50.

equal growth rates at $\omega_1/\omega \approx 2.15$, where the corresponding curves smoothly connect to each other. A similar property is also found at $R_v=50$ shown in Fig. 8(f).

Considering small values of R_v, we can study the modification of each disturbance mode for the parabolic velocity profile by computing the perturbation coefficients μ_{j2} according to Eq. (71) and (72), since $\mu_{j1}=0$. As shown in Fig. 8, there are no stable modes of the steady Poiseuille flow to be affected by the modulation to become the most unstable mode for $R_v<35$. Hence, it is enough to compute μ_{12}, whose real part is shown in Fig. 9. The numerical results are obtained from

$$\mathrm{Re}(\mu_{12}) = [\mathrm{Re}(\mu_1) - \mathrm{Re}(\mu_{10})]/\Delta^2 = \mathrm{Re}(\mu_1)/\Delta^2, \qquad (73)$$

since $\mathrm{Re}(\mu_1)=0$ for $R=R_c$, $\alpha=\alpha_c$. As shown in Fig. 9, the numerical results are in good agreement with the asymptotic ones for $R_v<10$. For larger R_v, the numerical results agree with the asymptotic solution only for high frequencies, while there is large discrepancy for low frequencies for the following two reasons. One is that the condition (31) is not valid anymore in this parameter range. The other is that the mean flow is strongly affected by the oscillatory wall suction/blowing so that the role of more higher-order terms becomes more important; thus Eq. (73), used to compute $\mathrm{Re}(\mu_{12})$, is no longer accurate.

The asymptotic results for $\mathrm{Re}(\mu_{12})$ shown in Fig. 9 are always positive, indicating the destabilizing effect of the modulation on the underlying flow. However, in an attempt to gain a further understanding of the mechanism by which the flow is destabilized, it is useful to study separately each term in Eq. (71). The variation of the three terms of $\mathrm{Re}(\mu_{12})$ is shown in Fig. 10. It is found that the first-order correction of the streamwise mean flow has a destabilizing effect for both high and low frequencies, as indicated by the positive value of $\mathrm{Re}(M_{11})$, and a stabilizing effect for $2.0<\omega_1/\omega<4.5$. The optimal stabilizing frequency is $\omega \approx \omega_1/3.35$. It is interesting to mention that the properties agree qualitatively with those of the channel flow modulated by an oscillatory pressure gradient, in which the mean flow can be obtained analytically, and is only composed of a steady part and a first-order oscillatory correction.[27] Since $\mathrm{Re}(M_{12})$ is always positive, the steady part of the second-order correction has a strongly destabilized effect on the flow. It is mainly because

TABLE I. The maximum growth rate $\mathrm{Re}(\mu_1)$ for $\alpha=1$, $R=5000$, $R_v=50$, $\omega=0.2$ for different number of Fourier modes M in (6) and different number of the collocation points N for the case of constant pressure gradient.

N	$M=1$	$M=2$	$M=5$	$M=10$
30	9.253129×10^{-3}	1.047563×10^{-2}	1.067871×10^{-2}	1.067876×10^{-2}
40	9.263003×10^{-3}	1.048517×10^{-2}	1.069547×10^{-2}	1.069550×10^{-2}
50	9.262982×10^{-3}	1.0648516×10^{-2}	1.069545×10^{-2}	1.069548×10^{-2}

TABLE II. The first four disturbance modes of the plane Poiseuille flow at $R=5772.22$, $\alpha=1.020\ 56$.

j	μ_{j0}			Symmetric (S) Antisymmetric (A)
1	0	+	0.269430i	S
2	−0.046 670	+	0.973519i	A
3	−0.0467 06	+	0.973543i	S
4	−0.058 792	+	0.327770i	A

of this term destabilizing the channel flow. The normal velocity has a stabilizing effect for $\omega_1/\omega<3.1$ and a destabilizing effect for the other range of ω_1/ω. We have also carried out a series of calculations, in which the mean streamwise velocity $U(y,t)$ is replaced artificially by the parabolic profile $1-y^2$ while the normal velocity remains unchanged. The real part of the first Floquet exponent is negative for a certain range of these parameters, which suggests the stabilizing effect of the normal velocity. Since such a flow configuration has no more physical meaning, the results are not given here. However, the stabilizing effects of the first-order correction of the mean flow and the normal velocity are not strong enough to overwhelm the destabilizing effect of the second-order term. So, the oscillatory wall suction/blowing has a totally destabilizing effect.

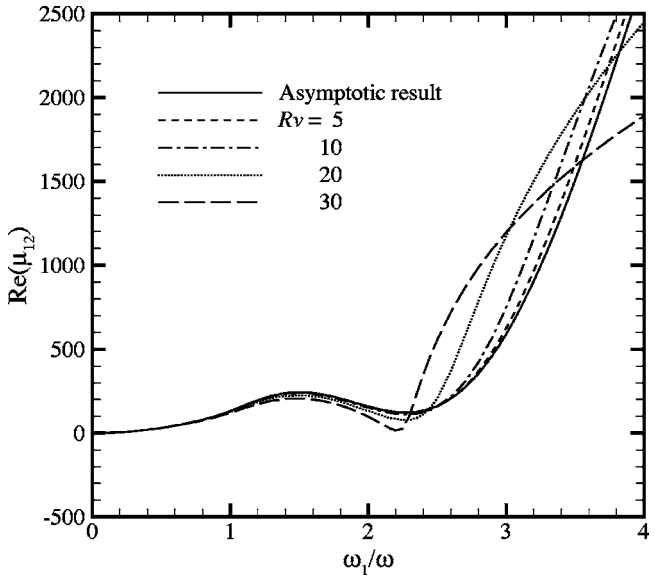

FIG. 9. Variation of $\mathrm{Re}(\mu_{12})$ as a function of ω_1/ω for various values of R_v at $R=5772.22$, $\alpha=1.020\ 56$.

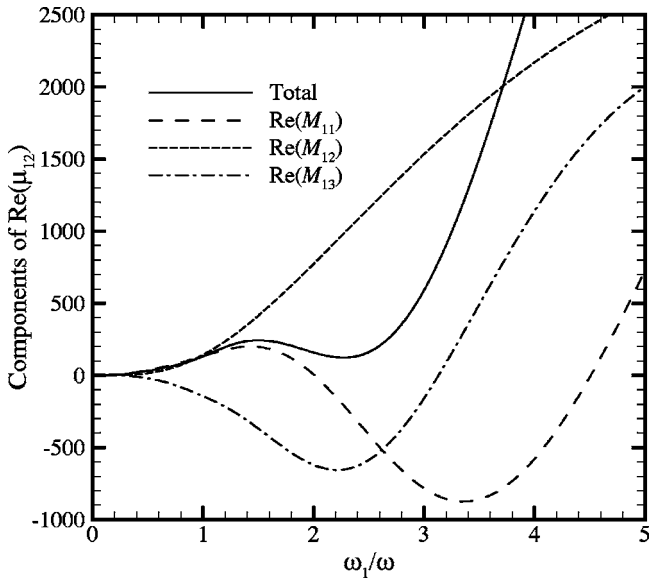

FIG. 10. Profiles of the real part of each term in Eq. (71) for the first disturbance mode as a function of ω_1/ω at $R=5772.22$, $\alpha=1.020\ 56$.

Based on the asymptotic analysis, we have calculated the perturbation coefficients μ_{j2} for the first four eigenvalues, the real part of which is shown in Fig. 11(a). The difference of $\mathrm{Re}(\mu_{22})$ and $\mathrm{Re}(\mu_{32})$ is too small to be identified. It is important to note that the fourth mode is so strongly destabilized by the oscillatory wall suction/blowing that it may even become the most unstable mode. These behaviors agree well with the numerical results described above. The variation of $\mathrm{Re}(\mu_{42}-\mu_{12})$ is shown in Fig. 11(b). The maximum value 1479 is reached at $\omega_1/\omega=2.5$. If we still assume that the asymptotic analysis is valid for large Δ, the growth rate of the fourth mode will be larger than that of the first mode at $\omega_1/\omega=2.5$ if

$$R_v > R_c\sqrt{\frac{\mathrm{Re}(\mu_{10}-\mu_{40})}{1479}} \approx 36, \tag{74}$$

which is in accordance with Fig. 8, even though the parameters R_v and ω in this case no longer satisfy the condition (31). Thus, the results shown in Fig. 8 can be qualitatively explained by the asymptotic theory.

C. Critical parameters

The results shown in Sec. IV B have demonstrated that the modulation of the oscillatory wall suction/blowing has an appreciable effect on the disturbance growth rate at the critical point $\alpha=\alpha_c$ and $R=R_c$ of steady Poiseuille flow. Further, it is also of interest to investigate the critical parameters and the relevant physics of the flow in a wide range of parameters. At the criticality, the real part of the Floquet exponent (i.e., μ_r) vanishes, while the imaginary part μ_i is nonzero generally, resulting in the Floquet mode being nonperiodic in time. In addition, if μ is a Floquet exponent, $\mu+in\omega$ is either, where n is an integer. Thus, the critical Reynolds number and wave number are discussed. To identify the critical parameters, extensive calculations by keeping Δ as a given value but changing R_v for each case have been carried out.

The critical Reynolds number R_{cr} and the corresponding disturbance wave number α_{cr} are plotted in Fig. 12 as a function of ω with constant Δ. Since large numbers of solution are needed to obtain these curves, several typical values of Δ are chosen. When the frequency approaches to infinity (or $\omega^{-1}\to 0$), it is found that R_{cr} and α_{cr} tend to $R_c=5772.22$ and $\alpha_c=1.020\ 56$, respectively. As ω^{-1} increases from zero, R_{cr} decreases to a local minimum around $\omega^{-1}=5$, then increases to some local maximum value that is less than R_c, and finally decreases again in the region of ω considered here. Figure 12(a) represents the destabilizing effect of the modulation

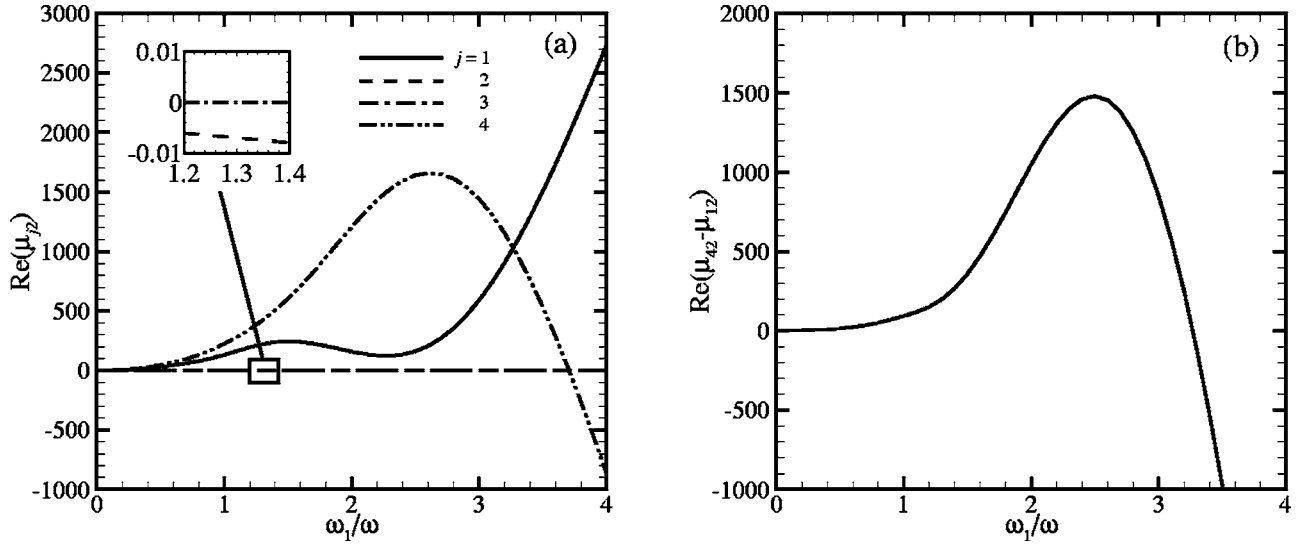

FIG. 11. Variation of (a) the real part of the perturbation coefficients μ_{j2} $(j=1,2,3,4)$ for the first four most unstable modes and (b) $\mathrm{Re}(\mu_{42}-\mu_{12})$ as a function of ω_1/ω at $R=5772.22$, $\alpha=1.020\,56$.

because $R_{cr}<R_c$. Furthermore, for sufficient low frequency, resulting in the leading term of the stability of the flow being a quasistatic problem, it is reasonably predicted that R_c may increase again since the channel flow can be stabilized by steady wall suction/injection.[9,20,21]

Note that the curves in Fig. 12 are continuous for small amplitude, e.g., $\Delta=0.001$, 0.002, and 0.004, but discontinuous for a large amplitude, e.g., $\Delta=0.005$ and 0.01. Figure 12(b) exhibits that the critical modes switch from high wave number disturbances to low ones at the discontinuous location. Here, the behavior of the neutral curve near the discontinuous location is discussed further. As a typical case for $\Delta=0.005$, the neutral curves for different frequencies around the discontinuous location (i.e., $\omega^{-1}=8.173$) are shown in Fig. 13(a). When $\omega^{-1}<8.173$, e.g., $\omega^{-1}=8$, one single neutral curve occurs. At $\omega^{-1}=8.173$ approximately, an additional neutral point S emerges in Fig. 13(a), which causes the discontinuity of the curves shown in Fig. 12. When ω^{-1} increases from 8.173 to 8.22, this point S expands to an isolated unstable region, which becomes larger and larger. At $\omega^{-1}=8.22$, the isolated curve just connects to the right-side neutral curve. When $\omega^{-1}>8.22$ (e.g., $\omega^{-1}=8.3$ and 8.5), only a single neutral curve exists again. To exhibit the variations of R and α, corresponding to the fold points of neutral curves in Fig. 13(a), the corresponding curves are shown in Fig. 13(b). Similarly, the existence of an isolated unstable region has also been found for the stability of a rotating doubly diffusive fluid layer[35] and the stability of a fluid layer on an oscillating plane.[36]

D. Channel flow with fixed flow rate

The stability characteristics of the channel flow with a fixed flow rate have also been investigated. Based on our extensive calculations, we have identified that the results are very similar to these of the channel flow driven by the con-

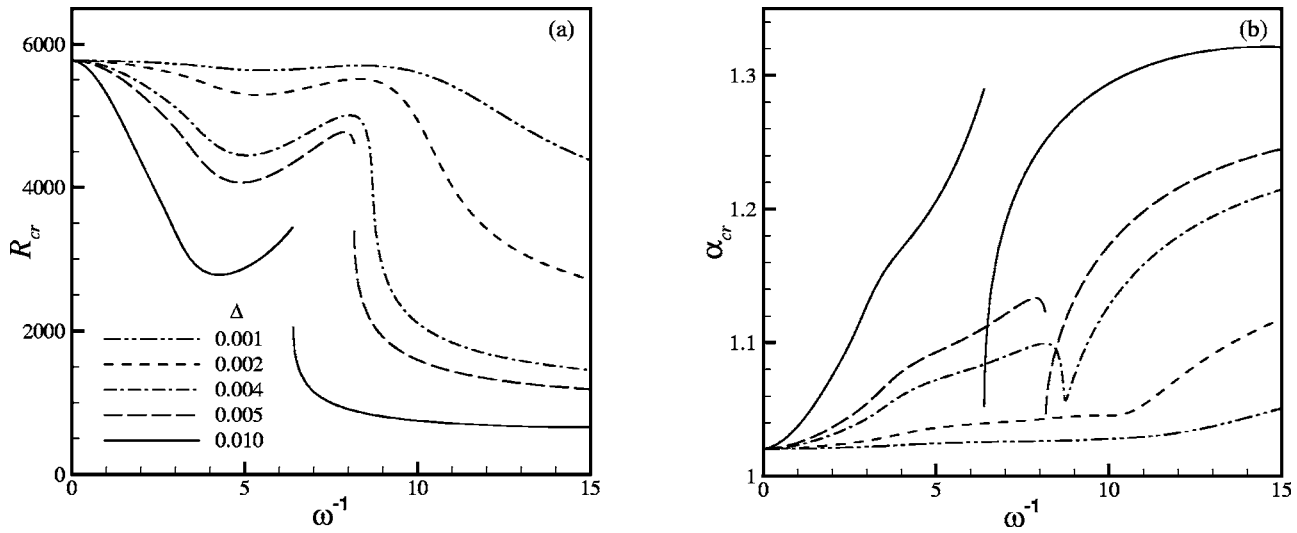

FIG. 12. Variation of (a) the critical Reynolds number R_{cr} and (b) the critical wave number α_{cr} as functions of ω^{-1} for typical values of Δ.

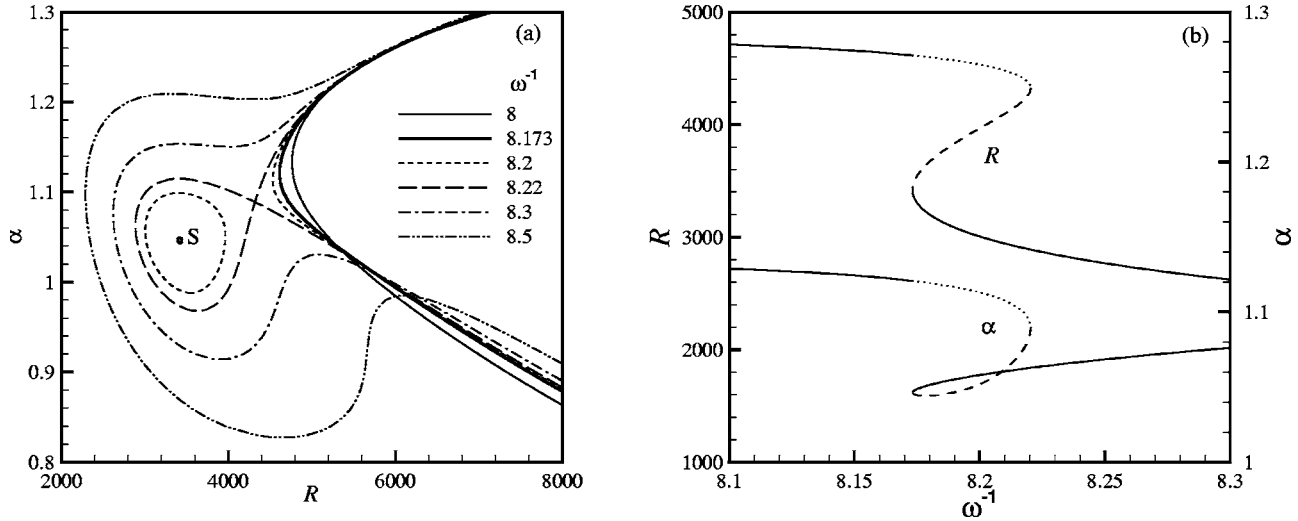

FIG. 13. (a) Typical neutral curves for ω^{-1} around the discontinuous location for $\Delta=0.005$ in Fig. 9; (b) the corresponding variation of R and α at the folds of the curves in (a), where the solid lines represent the critical Reynolds number and wave number, while the minimum of R and the corresponding α of the right-side neutral curves as well as the maximum of R and the corresponding α of the isolated curves (if exist) are denoted by the dotted and dashed lines, respectively.

stant pressure gradient described above, especially for small amplitude Δ. It is easy to understand the accordance of the results for the channel flows subject to both the constraint conditions when the amplitude Δ is sufficiently small. As discussed in Sec. II B, since the asymptotic formulations of the mean flow are identical to each other up to the first order. The difference appears in M_{j2}, which denotes the contribution of U_{20} on the oscillatory flow. Figure 14 shows the asymptotic results of $\mathrm{Re}(M_{12})$ to compare the effects of the modulation under two constraint conditions on the most unstable modes. Both the curves agree well with each other, even though a large discrepancy of U_{20} shown in Fig. 4 appears. As indicated by Herbert,[24] the velocity profile near the wall plays an important role on the stability of the channel flow modulated by an oscillatory pressure gradient. Thus, a reasonable explanation here is that the modification of the velocity profile near the wall will strongly affect the disturbances. If we introduce a new variable $\xi=1-|y|$ and expand the expression of U_{20} about $\xi=0$, the asymptotic approximations of U_{20} near the wall are obtained, i.e.,

$$U_{20}(\xi)=\mathrm{Re}\left(\frac{R^2}{\beta^2}\xi-\frac{R^2\coth\beta}{2\beta}\xi^2+\frac{R^2}{6}\xi^3\right)+O(\xi^4), \quad (75)$$

for a constant pressure gradient and

$$U_{20}(\xi)=\mathrm{Re}\left[\frac{R^2}{\beta^2}\left(\frac{3}{\beta^2}+1-\frac{3}{\beta}\coth\beta\right)\xi+\frac{R^2}{2\beta^3}\left(-\frac{3}{\beta}+3\coth\beta-\beta^2\coth\beta\right)\xi^2+\frac{R^2}{6}\xi^3\right]+O(\xi^4), \quad (76)$$

for a fixed flow rate. As $|\beta|\gg 1$ and $\coth\beta\approx 1$ for the parameters ω and R considered here, both Eqs. (75) and (76) can be reduced to

$$U_{20}(\xi)=R^2\,\mathrm{Re}\left(\frac{\xi}{\beta^2}-\frac{\xi^2}{2\beta}+\frac{\xi^3}{6}\right)+O(\xi^4)=\frac{1}{2}R^2\xi^2\left(\frac{\xi}{3}-\frac{1}{\sqrt{2\omega R}}\right)+O(\xi^4), \quad (77)$$

which leads to the consistency of the curves in Fig. 14. For the large amplitude considered in the present study, it is also found that there is no qualitative difference of the stability characteristics of the channel flows subject to both the constraint conditions (e.g., Fig. 5).

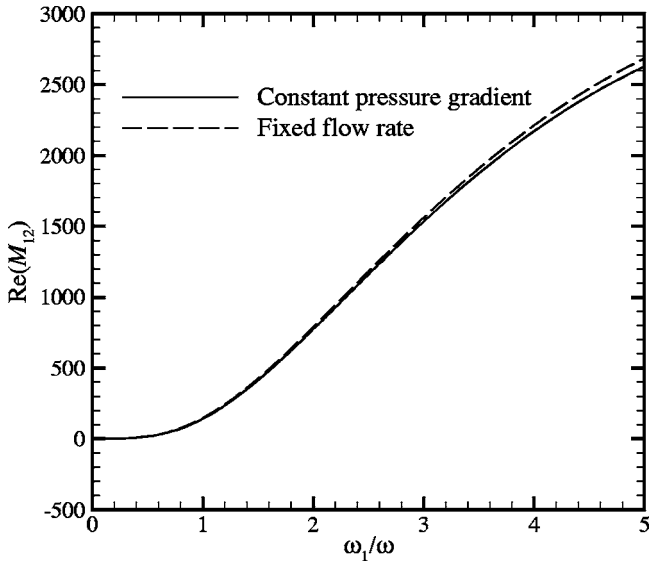

FIG. 14. Variation of $\mathrm{Re}(M_{12})$ as a function of ω_1/ω at $R=5772.22$, $\alpha=1.020\,56$.

V. CONCLUDING REMARKS

The effects of oscillatory wall suction/blowing on the stability of plane Poiseuille flow have been studied numerically and asymptotically using a linear stability analysis together with Floquet theory. The flows either driven by a con-

stant pressure gradient or constrained by a fixed flow rate are considered. It is revealed that the oscillatory wall suction/blowing induces the Stokes layer, which interacts with the disturbance shear wave and eventually affects the disturbance growth, and has a destabilizing effect on the channel flows.

The basic flow subject to the modulation is time periodic and composes multiple frequency components. If the channel flow is driven by a constant pressure gradient, the bulk mean velocity decreases compared with that of the pure Poiseuille flow. Considering weak oscillatory wall suction/blowing with small amplitude Δ, an asymptotic solution of the basic flow up to $O(\Delta^2)$ is obtained. The first-order modification is a temporal oscillatory solution with the same frequency as the modulation, and the second-order modification contains a steady term besides the oscillatory terms. Differences of the basic flows undergone by both the constraint conditions occur in the $O(\Delta^2)$ terms.

The stability problem is formulated into a time-dependent eigenvalue problem. The Floquet exponents, which guarantee the stability characteristics of the flow, are then obtained by solving the stability problem with a spectral collocation method. For the critical parameters $R=5772.22$ and $\alpha=1.020\,56$ of steady Poiseuille flow, the disturbance is unstable for most values of R_v and ω, indicating that the modulation of the oscillatory wall suction/blowing has a destabilizing effect on the underlying flow. It is also found that the disturbance can be stabilized in a limited range of parameters in the $R_v-\omega$ plane.

Further, in an extensive region of the parameters studied, the critical Reynolds number reduces and hence the flow is destabilized by the wall suction/blowing. In addition, the neutral curves become significantly complex compared with steady Poiseuille flow. In particular, isolated unstable regions occur in certain parameters.

An asymptotic expansion for the growth rate shows that the modification terms in $O(\Delta^2)$ are positive, indicating the destabilizing effect of the modulation. Further, based on the expansion, the terms in the $O(\Delta^2)$ can be reasonably divided into three parts, including the contributions of the first-order correction of the streamwise mean flow, the steady part of the second-order correction of the streamwise mean flow, and the normal mean flow, respectively. Then, it is revealed that the stabilizing effects of the first-order correction of the mean flow and the normal velocity are not strong enough to overwhelm the destabilizing effect of the second-order term. Thus, the oscillatory wall suction/blowing has totally a destabilizing effect on the channel flows.

Based on the asymptotic analysis, we can understand that the velocity profile near the wall would strongly affect the disturbances. Since the velocity modifications near the wall for both the constraint conditions approach together, it is reasonably found that there are the similar stability characteristics of the channel flows with either the driven pressure gradient or the flow rate constant.

ACKNOWLEDGMENTS

This work was supported by the National Natural Science Foundation of China (No. 90405007, No. 10125210), the Innovation Project of the Chinese Academy of Sciences (No. KJCX-SW-L04), and the Hundred Talents Program of the Chinese Academy of Sciences. The authors thank Professor D.-J. Sun and referees for valuable comments.

[1] S. A. Orszag, "Accurate solution of the Orr-Sommerfeld stability equation," J. Fluid Mech. **50**, 689 (1971).
[2] A. Cabal, J. Szumbarski, and J. M. Floryan, "Stability of flow in a wavy channel," J. Fluid Mech. **457**, 191 (2002).
[3] J. M. Floryan, "Stability of wall-bounded shear layers in the presence of simulated distributed surface roughness," J. Fluid Mech. **335**, 29 (1997).
[4] J. Luo and X. Wu, "Influence of small imperfections on the stability of plane Poiseuille flow: A theoretical model and direct numerical simulation," Phys. Fluids **16**, 2852 (2004).
[5] J. M. Floryan, "Vortex instability in a diverging-converging channel," J. Fluid Mech. **482**, 17 (2003).
[6] J. M. Floryan, J. Szumbarski, and X. Wu, "Stability of flow in a channel with vibrating walls," Phys. Fluids **14**, 3927 (2002).
[7] S. Selvarajan, E. G. Tulapurkara, and V. Vasanta Ram, "Stability characteristics of wavy walled channel flows," Phys. Fluids **11**, 579 (1999).
[8] H. Zhou, R. J. Martinuzzi, R. E. Khayat, A. G. Straatman, and E. Abu-Ramadan, "Influence of wall shape on vortex formation in modulated channel flow," Phys. Fluids **15**, 3114 (2003).
[9] J. H. Fransson and P. H. Alfredsson, "On the hydrodynamic stability of channel flow with cross flow," Phys. Fluids **15**, 436 (2003).
[10] J. J. Szumbarski and J. M. Floryan, "Channel flow instability in presence of weak distributed surface suction," AIAA J. **38**, 372 (2000).
[11] T. R. Bewley and S. Liu, "Optimal and robust control and estimation of linear paths to transition," J. Fluid Mech. **365**, 305 (1998).
[12] B. F. Farrel and P. J. Ioannou, "Turbulence suppression by active control," Phys. Fluids **8**, 1257 (1996).
[13] S. S. Joslin, J. L. Speyer, and J. Kim,"A systems theory approach to the feedback stabilization of infinitesimal and finite-amplitude disturbances in plane Poiseuille flow," J. Fluid Mech. **332**, 157 (1997).
[14] T. Bewley, P. Moin, and R. Temam, "DNS-based predictive control of turbulence: an optimal benchmark for feedback algorithms," J. Fluid Mech. **447**, 179 (2001).
[15] M. Högberg, T. R. Bewley, and D. S. Henningson, "Relaminarization of $\mathrm{Re}_\tau=100$, turbulence using gain scheduling and linear state-feedback control," Phys. Fluids **15**, 3572 (2003).
[16] H. Choi, P. Moin, and J. Kim, "Active turbulence control for drag reduction in wall bounded flows," J. Fluid Mech. **262**, 75 (1994).
[17] Y. Sumitani and N. Kasagi, "Direct numerical simulation of turbulent transport with uniform wall injection and suction," AIAA J. **33**, 1220 (1995).
[18] T. H. Hughes and W. H. Reid, "On the stability of the asymptotic suction boundary-layer profile," J. Fluid Mech. **23**, 715 (1965).
[19] L. M. Hocking, "Non-linear instability of the asymptotic suction velocity profile," Q. J. Mech. Appl. Math. **28**, 341 (1975).
[20] F. D. Hains, "Stability of plane Couette-Poiseuille flow with crossflow," Phys. Fluids **14**, 1620 (1971).
[21] D. M. Sheppard, "Hydrodynamic stability of the flow between parallel porous walls," Phys. Fluids **15**, 241 (1972).
[22] S. H. Davis, "The stability of time-periodic flows," Annu. Rev. Fluid Mech. **8**, 57 (1976).
[23] C. E. Grosch and H. Salwen,"The stability of steady and time-dependent plane Poiseuille flow," J. Fluid Mech. **34**, 177 (1968).
[24] D. M. Herbert, "The energy balance in modulated plane Poiseuille flow," J. Fluid Mech. **56**, 73 (1972).
[25] C. C. Lin, *The Theory of Hydrodynamic Stability* (Cambridge University Press, Cambridge, 1954).
[26] P. Hall, "The stability of Poiseuille flow modulated at high frequencies," Proc. R. Soc. London, Ser. A **344**, 453 (1975).
[27] C. H. von Kerczek,"The instability oscillatory plane Poiseuille flow," J. Fluid Mech. **116**, 91 (1982).
[28] B. A. Singer, J. H. Ferziger, and H. L. Reed, "Numerical simulations of transition in oscillatory plane channel flow," J. Fluid Mech. **208**, 45 (1989).
[29] A. G. Straatman, R. E. Khayat, E. Haj-Qasem, and D. A. Steinman, "On

the hydrodynamic stability of pulsatile flow in a plane channel," Phys. Fluids **14**, 1938 (2002).
[30]E. A. Coddington and N. Levenson, *Theory of Ordinary Differential Equations* (McGraw-Hill, New York, 1955).
[31]C. von Kerczek and S. H. Davis, "Linear stability theory of oscillatory Stokes layers," J. Fluid Mech. **62**, 753 (1974).
[32]J. A. C. Weideman and S. C. Reddy, "A MATLAB differentiation matrix suite," ACM Trans. Math. Softw. **26**, 465 (2000).
[33]M. Högberg, T. R. Bewley, and D. S. Henningson, "Linear feedback control and estimation of transition in plane channel flow," J. Fluid Mech. **481**, 149 (2003).
[34]A. Bottaro, P. Corbett, and P. Luchini, "The effect of base flow variation on flow stability," J. Fluid Mech. **476**, 293 (2003).
[35]A. J. Pearlstein, "Effect of rotation on the stability of a doubly diffusive fluid layer," J. Fluid Mech. **103**, 389 (1981).
[36]A. C. Or, "Finite-wavelength instability in a horizontal liquid layer on an oscillating plane," J. Fluid Mech. **335**, 213 (1997).